Experimental Retrieval of Target Structure Information from Laser-Induced Rescattered Photoelectron Momentum Distributions

M. Okunishi,[1] T. Morishita,[2,3] G. Prümper,[1] K. Shimada,[1] C. D. Lin,[4] S. Watanabe,[2] and K. Ueda[1,*]

[1]*Institute of Multidisciplinary Research for Advanced Materials, Tohoku University, Sendai 980-8577, Japan*

[2]*Department of Applied Physics and Chemistry, University of Electro-Communications, 1-5-1 Chofu-ga-oka, Chofu-shi, Tokyo 182-8585, Japan*

[3]*PRESTO, Japan Science and Technology Agency, Kawaguchi, Saitama 332-0012, Japan*

[4]*Department of Physics, Kansas State University, Manhattan, Kansas 66506, USA*

(Received 6 December 2007; published 9 April 2008)

We have measured two-dimensional photoelectron momentum spectra of Ne, Ar, and Xe generated by 800-nm, 100-fs laser pulses and succeeded in identifying the spectral ridge region (back-rescattered ridges) which marks the location of the returning electrons that have been backscattered at their maximum kinetic energies. We demonstrate that the structural information, in particular the differential elastic scattering cross sections of the target ion by free electrons, can be accurately extracted from the intensity distributions of photoelectrons on the ridges, thus effecting a first step toward laser-induced self-imaging of the target, with unprecedented spatial and temporal resolutions.

DOI: 10.1103/PhysRevLett.100.143001 PACS numbers: 32.80.−t, 32.80.Rm, 33.20.Xx

In recent years, the interaction of atoms and molecules with intense laser fields continues to receive wide interest with the discovery of many new exciting phenomena (see, for example, [1] and references therein). When an atom or a molecule is exposed to an optical field whose magnitude matches the intra-atomic and intramolecular Coulombic fields, the atom or the molecule is first tunnel ionized, releasing an electron. This electron is placed in the oscillating electric field of the laser and may be driven back to its parent ion. This re-encounter may incur various elastic and inelastic electron-ion collision phenomena. These elementary processes form the core of the rescattering theory [2,3] and initiate many interesting laser-induced phenomena. Among them, the first exciting one may be the generation of attosecond pulses and the subsequent emergence of ''attosecond science'' [4–6]. The second exciting one, which has been widely discussed (see [7,8] and references therein) but not yet been implemented, is the possibility of using the returning electron for self-imaging the target, as it may collide with the target ion.

When a laser-induced photoelectron is driven back to recollide with the target ion, structural information of the target can be extracted from the recombination of the electron and ion. In a recent paper, Itatani *et al.* reported that the outermost molecular orbital of the N_2 molecule can be extracted from the high-order harmonic generation spectra using the tomographic procedure [9]. This inspiring idea, together with an exploratory experimental result, has generated a wave of excitement. However, their extracted orbital wave function, even though impressive, relies on a number of unchecked assumptions [10–12]. To make their idea as a practical tool for retrieving structural information it still awaits a careful theoretical investigation of the underlying assumptions.

Along this direction, it has been shown recently by Morishita *et al.* [13,14] that differential elastic scattering cross sections of the target ion by free electrons can be accurately extracted from laser-induced photoelectron momentum spectra, a method dubbed the ''light-induced electron microscope.'' Their conclusion was drawn from accurate numerical results by solving the time-dependent Schrödinger equation of atoms in intense laser fields. Since differential elastic scattering cross sections by free electrons are the conventional methods for investigating the structure of atoms and molecules, the light-induced electron microscope offers the possibility of determining their structure using lasers, with the added benefit of achieving femto- to subfemtosecond temporal resolutions offered by the short laser pulses.

In the present Letter, we present the first experimental demonstration of the prediction of Morishita *et al.* Namely, we measured the angular distributions of laser-induced backscattered photoelectrons of Ne, Ar, and Xe atoms, using laser pulses at wavelength of 800 nm and pulse width of 100 fs, and extracted the elastic differential scattering cross sections of the target ions Ne^+, Ar^+, and Xe^+ by free electrons, by applying the recipe of Morishita *et al.*. We illustrated that the elastic scattering cross sections of these target ions can indeed be extracted from the angular distributions of the measured photoelectrons. While the present conclusion is derived from atomic targets with 100-fs laser pulses, the procedure is expected to apply to molecular targets exposed to few-cycle pulses as well.

Let us describe the experimental method first. In our experiments, we detected electrons using a 264-mm-long linear time-of-flight (TOF) spectrometer with a limited detection angle ($\sim 0.0014 \times 4\pi$ sr). The fundamental output (800 nm) from an amplified Ti:Sapphire laser system (pulse width of 100 fs, repetition rate of 1 kHz) was used as the ionizing radiation. The 2–3 mm diameter laser beam was focused by an $f = 60$ mm lens to a field free location between two grounded electrodes comprising graphite-

coated Al with 80% transmission Cu mesh. Ar, Kr or Xe gas was effusively introduced: a typical working pressure is in the range of $(3–7) \times 10^{-6}$ mb, whereas the base pressure is less than 10^{-10} mb.

To perform the angular distribution measurement of the photoelectrons, the polarization direction of the laser was varied using a $\lambda/2$ plate. This plate was rotated with a constant speed of exactly one rotation per minute and thus the laser polarization makes one full turn in every 30 s. The total data acquisition time was typically 2–4 hours, averaging over several hundred rotations of the electric vector. No synchronization of the rotation and the laser pulses was used. Instead we recorded a marker signal for the position of the $\lambda/2$ plate as a function of the laser shots. From this signal the laser polarization direction for each laser shot was derived. Only electrons ejected in the direction of the TOF spectrometer were detected by tandem microchannel plates.

To obtain the peak laser intensity at the ionization point, we measured the ratio of Xe^{2+} to Xe^{+} as a function of the incident laser power and, using the results of Talebpour *et al.* [15] as reference data, we established the relation between the peak laser intensity and the reading of the laser power measured by the power meter in the nonsaturation regime well below 10^{14} W/cm^2. The peak laser intensity cited in this paper is based on the linear extrapolation of this intensity scale. Our measurements presented below are recorded at ~3.5, ~2.3, and $\sim 1.5 \times 10^{14}$ W/cm^2 for Ne, Ar, and Xe, respectively, in this scale. We note that these intensities are already in the saturation regime, and the contributions to the experimental ionization spectra come from the wide range of laser intensities lower than these values due to the volume focusing effect [16].

The electron energy calibration was made with reference to the multiphoton ionization of Xe atoms in the kinetic energy region of less than 10 eV. Comparing the time origin of the TOF spectrometer from this calibration with the measured one, we estimated that the error of the energy scale in our data is <5%. The efficacy of our high resolution electron spectroscopy technique to study strong field molecular dynamics has been recently demonstrated [17–19]. Further details of the experimental setup and procedure are given elsewhere [20,21].

Figure 1 depicts the typical electron spectra measured with Xe at laser intensity 1.5×10^{14} W/cm^2, at angles 0°, 30°, 60°, and 90°, relative to the polarization vector. In the figure, two particular energies, $2U_p^{(\mathrm{eff})}$ and $10U_p^{(\mathrm{eff})}$, are marked, where $U_p^{(\mathrm{eff})}$ is the effective ponderomotive potential determined by the cutoff of the experimental spectra. According to the classical estimate, an electron can reach up to $2U_p^{(\mathrm{eff})}$ if it is released by the laser field alone. It can reach up to $10U_p^{(\mathrm{eff})}$ if it returns and is then further backscattered by the parent ion [22,23]. From the electron spectra in Fig. 1, it is clear that rescattering contribution becomes less for larger angles. Characteristic angular distributions of high-energy photoelectrons have been observed for Kr and Xe [22] and analyzed using different theoretical approaches [23–25]. However, direct connection between laser-induced photoelectron angular distributions of neutral atoms with the elastic backscattering of target atomic ions by free electrons was first established quantitatively by Morishita *et al.* [13,14].

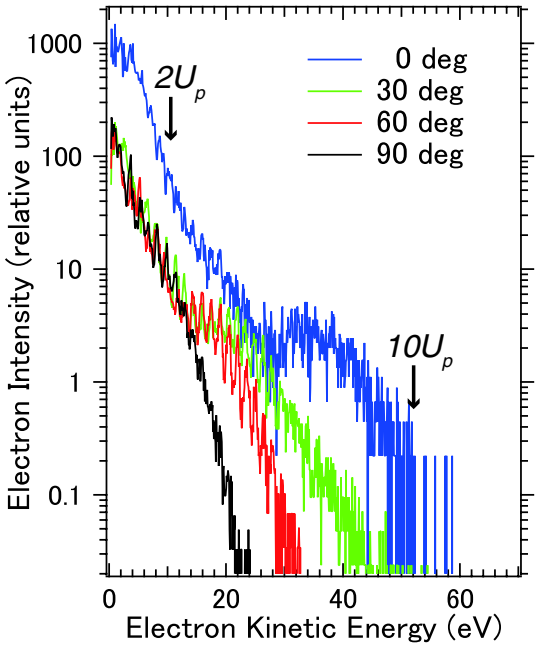

FIG. 1 (color online). Laser-induced photoelectron spectrum for Xe, at laser intensity 1.5×10^{14} W/cm^2 at angles 0°, 30°, 60°, and 90°, relative to the polarization vector.

To identify the contribution from high-energy rescattered electrons, we plot in Fig. 2 two-dimensional (2D) momentum distributions for high-energy electrons from Ne, Ar, and Xe, at the laser intensities of 3.5, 2.3, and 1.5×10^{14} W/cm^2, respectively. We have chosen the horizontal axis to be along the direction of the light polarization and the vertical axis along any direction perpendicular to it (due to cylindrical symmetry of the linearly polarized light; see, e.g., Maharjan *et al.* [26]). In Fig. 2 the photoelectron distributions for Ne, Ar, and Xe are quite different, particularly along the half-circular ridges marked with dashed lines; see Fig. 2.

To understand these circular ridges, some theoretical remarks are in order. They represent the electron that has been rescattered into the backward directions by the parent ion. Thus they are called "back-rescattered ridges" (BRR) electrons [13,14]. The BRR on the right (left) is from the electron that travels away to the right (left) initially, returns to the ion, and then is rescattered back to the right (left). The position of the BRR in the 2D momentum space can be expressed as

$$\boldsymbol{p} = \mp A_r \hat{\boldsymbol{p}}_z + p \hat{\boldsymbol{p}}_r, \tag{1}$$

where the first term is the momentum gain as the electron propagates from the time of the backscattering to the end of

the laser pulse. Here, A_r is the vector potential whose magnitude is related to the effective ponderomotive energy by $U_p^{(\mathrm{eff})} = A_r^2/4$. (Atomic units are used such that the vector potential has the units of electron momentum.) The second term represents the backscattering of the electron into direction $\hat{\boldsymbol{p}}_r$. The magnitude of the momentum p is related to the effective ponderomotive energy by $3.17U_p^{(\mathrm{eff})} = p^2/2$. Thus we have $p = 1.26A_r$. Note that this association of A_r and p also identifies the location of the effective center of the circular ring as a function of the field strength. The decomposition into parallel and perpendicular photoelectron momenta gives

$$p_{\parallel} = \pm A_r - p\cos\theta_r, \qquad p_{\perp} = p\sin\theta_r, \tag{2}$$

where θ_r is the backscattering angle, ranging from 90° to 180°.

In Fig. 3, we replot the photoelectron yields along BRR as a function of the backscattering angle θ_r. Here we plot the photoelectron yields within the bins of $p = 1.7 \pm 0.05$ a.u., 1.3 ± 0.05 a.u., and 1.1 ± 0.05 a.u. for Ne, Ar, and Xe, respectively. These values of p correspond to the effective kinetic energy $3.17U_p^{(\mathrm{eff})}$ of the returning electrons 39, 23, and 16.5 eV for Ne, Ar, and Xe, respectively. We comment that these electrons have much lower energies in comparison to the tens to hundreds of keV electrons used for electron diffraction.

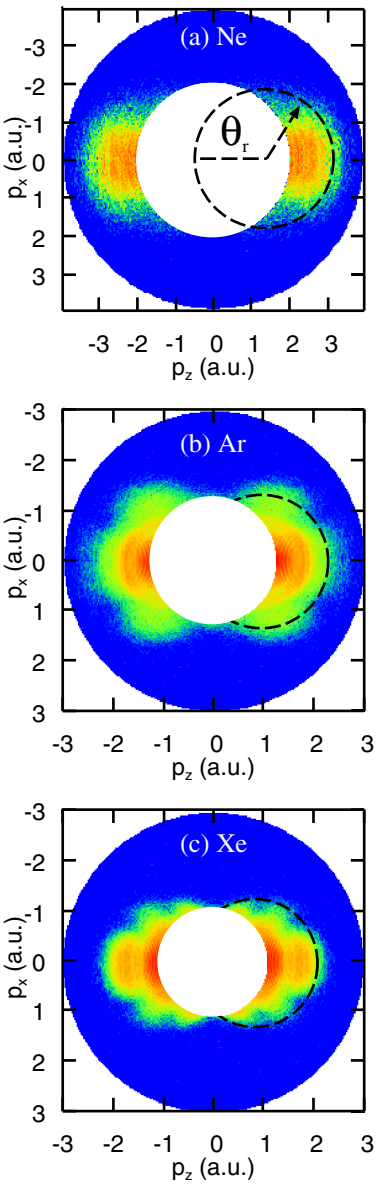

FIG. 2 (color online). 2D photoelectron momentum spectra: (a) for Ne at the laser intensity 3.5×10^{14} W/cm^2, (b) for Ar at the laser intensity 2.3×10^{14} W/cm^2, (c) for Xe at the laser intensity 1.5×10^{14} W/cm^2. The images are plotted in logarithmic scale. The experimental ridge is shown in a dashed circle for each target atom.

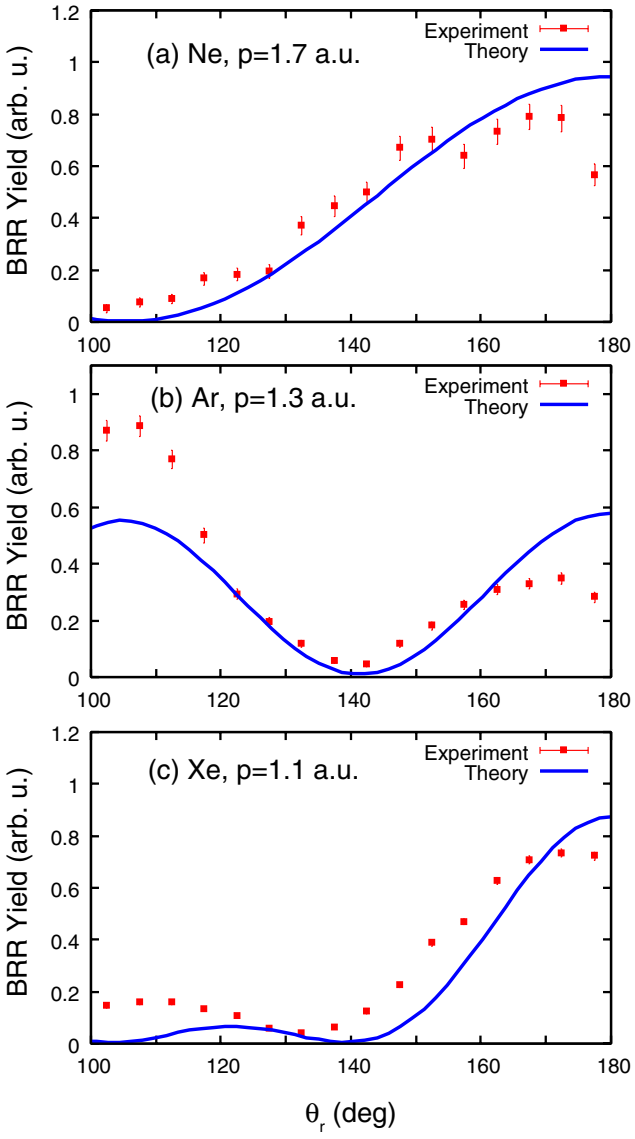

FIG. 3 (color online). Angular distributions of photoelectrons along the BRR compared to the differential elastic scattering cross sections of the target ion: (a) for Ne, (b) for Ar, and (c) for Xe.

Comparing the extracted photoelectron momentum spectra with the calculated differential elastic cross sections of the target ion by a free electron at energy $E = p^2/2$, we found very reasonable agreement between the two results for each target atom. In particular, a very clear minimum in the differential cross section can be seen in Ar and Xe, while the monotonous decrease in the cross sections as the angle decreases, with a possible additional minimum at about 110°, can be seen for Ne. In calculating elastic scattering cross sections, we used a model potential to approximate the interaction between the active electron with the ion core [16]. We use the form of the effective charge of the potentials in Ref. [27], $Z_{\mathrm{eff}}(r) = -1 + a_1 e^{-a_2 r} + a_3 r e^{-a_4 r} + a_5 e^{-a_6 r}$. The actual numbers of parameter sets $\{a_i\}$ are listed in Ref. [27] for Ne and Ar, and $a_1 = 51.356$, $a_2 = 2.112$, $a_3 = -99.927$, $a_4 = 3.737$, $a_5 = 1.644$, and $a_6 = 0.431$ are used for Xe. These comparisons illustrate that laser-induced momentum images on the BRR can be used to obtain elastic scattering cross sections of a free electron by the target ion. The minima can be interpreted as due to the interference between the scattering amplitudes corresponding to Coulombic potential and the remaining short-range potential as demonstrating the use of the screened Coulomb potential to describe the electron-ion interaction [28]. Alternatively, one can view it as evidence of diffraction of electrons scattered by the potential.

Careful inspection reveals some discrepancies between the theoretical curve and the experimental points for each target (Fig. 3). These differences mainly stem from the fact that the BRR cross sections at smaller scattering angles are ''contaminated'' by rescattering into the forward directions from the other half cycle; see Ref. [13]. For scattering angles around 180°, the discrepancy may possibly arise from the many-electron effect on the elastic scattering cross sections which has not been treated in the single-electron model. In the future, additional differential cross sections will be obtained experimentally by using different laser intensities and/or different wavelengths. From several sets of such data, the structure can be retrieved by finding the parameters in the model potential that best fit the experimental differential cross sections.

In summary, we have demonstrated that the angular anisotropy of the electron emission along the BRR directly reflects differential elastic cross sections of the target ion by a free electron. This conclusion has far-reaching implications since electron scattering is a powerful tool for determining the structure of molecules in the traditional energy-domain measurements. For molecules, a multicenter model potential is quite adequate to describe the elastic scattering by the electrons. Such a potential also has information on the positions of all the atomic centers. This implies that infrared lasers can be employed to probe the structure of molecules. For few-cycle infrared lasers, the rescattering of the electrons with the parent ions occurs within the order of 1 femtosecond and with attosecond temporal resolution [29]. Thus few-cycle infrared lasers can handily achieve subfemtosecond temporal resolution, and they may serve as efficient ultrafast cameras for imaging physical, chemical, and biological systems where the system is undergoing rapid structural change.

This work was supported in part by the PRESTO program of the Japan Science and Technology Agency (JST), by the budget for ''Promotion of X-Ray Free Electron Laser Research'' from the Ministry of Education, Culture, Sports, Science and Technology (MEXT), by Grants-in-Aid for Scientific Research from the Japanese Society for the Promotion of Science (JSPS), by the 21st Century COE program on ''Coherent Optical Science,'' and by a JSPS bilateral joint program between the U.S. and Japan. C. D. L. is supported by the Chemical Sciences, Geosciences and Biosciences Division, Office of Basic Energy Sciences, Office of Science, U.S. Department of Energy.

*ueda@tagen.tohoku.ac.jp

[1] *Progress in Ultrafast Intense Laser Science*, edited by K. Yamanouchi, S. L. Chin, P. Agostini, and G. Ferrante (Springer, Berlin, 2006).
[2] K. Schafer *et al.*, Phys. Rev. Lett. **70**, 1599 (1993).
[3] P. B. Corkum, Phys. Rev. Lett. **71**, 1994 (1993).
[4] M. Drescher *et al.*, Nature (London) **419**, 803 (2002).
[5] M. Drescher and F. Krausz, J. Phys. B **38**, S727 (2005).
[6] T. Morishita, S. Watanabe, and C. D. Lin, Phys. Rev. Lett. **98**, 083003 (2007).
[7] S. X. Hu and L. A. Collins, Phys. Rev. Lett. **94**, 073004 (2005).
[8] S. N. Yurchenko *et al.*, Phys. Rev. Lett. **93**, 223003 (2004).
[9] J. Itatani *et al.*, Nature (London) **432**, 867 (2004).
[10] V.-H. Le *et al.*, Phys. Rev. A **76**, 013414 (2007).
[11] S. Patchkovskii *et al.*, Phys. Rev. Lett. **97**, 123003 (2006).
[12] J. Levesque *et al.*, Phys. Rev. Lett. **98**, 183903 (2007).
[13] T. Morishita *et al.*, Phys. Rev. Lett. **100**, 013903 (2008).
[14] T. Morishita *et al.*, New J. Phys. **10**, 025011 (2008).
[15] A. Talebpour *et al.*, J. Phys. B **30**, 1721 (1997).
[16] T. Morishita *et al.*, Phys. Rev. A **75**, 023407 (2007).
[17] T. Hatamoto *et al.*, Chem. Phys. Lett. **439**, 296 (2007).
[18] M. Okunishi *et al.*, J. Chem. Phys. **127**, 064310 (2007).
[19] D. Mathur *et al.*, J. Phys. Chem. A **111**, 9299 (2007).
[20] K. Ueda *et al.*, Proc. SPIE **6726**, 672603 (2007).
[21] T. Hatamoto *et al.*, Phys. Rev. A **75**, 061402(R) (2007).
[22] B. Yang *et al.*, Phys. Rev. Lett. **71**, 3770 (1993).
[23] G. G. Paulus *et al.*, J. Phys. B **27**, L703 (1994).
[24] M. Lewenstein *et al.*, Phys. Rev. A **51**, 1495 (1995).
[25] S. Dionissopoulou *et al.*, Phys. Rev. A **55**, 4397 (1997).
[26] C. M. Maharjan *et al.*, J. Phys. B **39**, 1955 (2006).
[27] X. M. Tong and C. D. Lin, J. Phys. B **38**, 2593 (2005).
[28] A. Messiah, *Quantum Mechanics* (John Wiley & Sons, New York, 1958).
[29] H. Niikura *et al.*, Nature (London) **421**, 826 (2003).